Automatica 46 (2010) 701–707

Contents lists available at ScienceDirect

Automatica

journal homepage: www.elsevier.com/locate/automatica

Brief paper

Integrated direct/indirect adaptive robust contouring control of a biaxial gantry with accurate parameter estimations[☆]

Chuxiong Hu[a], Bin Yao[a,b,*], Qingfeng Wang[a]

[a] The State Key Laboratory of Fluid Power Transmission and Control, Zhejiang University, Hangzhou, 310027, China

[b] School of Mechanical Engineering, Purdue University, West Lafayette, IN 47907, USA

ARTICLE INFO

Article history:
Received 15 April 2009
Received in revised form
20 August 2009
Accepted 8 January 2010
Available online 2 March 2010

Keywords:
Contouring control
Linear motor
Adaptive control
Parameter estimation
Robust control

ABSTRACT

This paper presents an integrated direct/indirect adaptive robust contouring controller (DIARC) for an industrial biaxial high-speed gantry that achieves not only excellent contouring performance but also accurate parameter estimations for secondary purposes such as machine health monitoring and prognosis. Contouring control problem is first formulated in a task coordinate frame. A physical model-based indirect-type parameter estimation algorithm is then developed to obtain accurate on-line estimates of unknown model parameters. A DIARC controller possessing dynamic-compensation-like fast adaptation is subsequently constructed to preserve the excellent transient and steady-state contouring performance of the direct adaptive robust controller (DARC) designs. The proposed DIARC along with previously developed DARC contouring controllers are implemented on a high-speed industrial biaxial gantry to test their achievable performance in practice. Comparative experimental results verify the improved contouring performance and the accurate physical parameter estimates of the proposed DIARC algorithm.

1. Introduction

To have a higher productivity and a better quality of the product produced, modern mechanical systems in manufacturing applications are often required to follow certain desired contours precisely with high speeds. The degradation of contouring performance (Li, 1999) could be due to either the lack of coordination among multi-axes motions (Chiu & Tomizuka, 2001) or the effects of model uncertainties/disturbances such as the change of payload inertia, friction (Lu, Yao, Wang, & Chen, 2009; Xu & Yao, 2008), and ripple forces (Lu, Chen, Yao, & Wang, 2008). The former is referred to as the coordinated contouring control problem (Koren, 1980) and the later as the disturbance rejection/compensation. Both problems have been extensively studied in the literature. Specifically, earlier researches on the coordinated contouring control use the cross-coupled control (CCC) strategy (Koren, 1980). Later on, the contouring control problem is formulated in a task coordinate frame by using either (i) the concept of generalized curvilinear coordinates introduced in Yao, Chan, and Wang (1994), as done in Chiu and Yao (1997) and Xu and Yao (2000), or (ii) the *locally* defined coordinates "attached" to the desired contour proposed in Chiu and Tomizuka (2001). Since then many contouring control schemes based on task coordinate approaches have been reported (Cheng & Lee, 2007; Chen & Lin, 2008). However, all these latest publications on coordinated control techniques cannot explicitly deal with parametric uncertainties and uncertain nonlinearities. As a result, they are often insufficient when stringent contouring performance is of concern as actual systems are always subjected to certain model uncertainties and disturbances.

During the past decade, an adaptive robust control (ARC) framework has been developed in Yao (1997) and Yao and Tomizuka (1996, 2001) to provide a rigorous theoretic framework for the precision motion control of systems with both parametric uncertainties and uncertain nonlinearities. The desired compensation ARC (DCARC) strategy has also been proposed in Yao (1998) to reduce the effect of measurement noises. In Xu and Yao (2001a,b), the proposed ARC strategy is experimentally tested on an *epoxy* core linear motor. Global stability is also guaranteed even in the presence of actuator saturation and short duration of very large disturbances (Hong & Yao, 2007).

In Hu, Yao, and Wang (in press-a), the ARC strategy (Yao, 1997) and the task coordinate frame approach in Chiu and Tomizuka

☆ The work is supported in part by the US National Science Foundation (Grant No. CMS-0600516) and in part by the National Natural Science Foundation of China (NSFC) under the Joint Research Fund for Overseas Chinese Young Scholars (Grant No. 50528505) and the Ministry of Education of China through a Chang Jiang Chair Professorship. The material in this paper was not presented at any conference. This paper was recommended for publication in revised form by Associate Editor Yoshikazu Hayakawa under the direction of Editor Toshiharu Sugie.

* Corresponding author at: School of Mechanical Engineering, Purdue University, West Lafayette, IN 47907, USA. Tel.: +1 765 494 7746; fax: +1 765 494 0539.
E-mail addresses: fyfox.hu@gmail.com (C. Hu), byao@purdue.edu (B. Yao), qfwang@zju.edu.cn (Q. Wang).

0005-1098/$ – see front matter © 2010 Elsevier Ltd. All rights reserved.
doi:10.1016/j.automatica.2010.01.022

(2001) have been integrated to develop a high performance contouring controller for high-speed machines. The effect of cogging forces and velocity measurement noises is also carefully addressed in Hu, Yao, and Wang (in press-b) with excellent contouring performance seen in implementation. However, as other direct ARC controllers (Hong & Yao, 2007; Lu et al., 2008; Xu & Yao, 2001a,b), the parameter estimates in experiments rarely approach to their true values, even when the persistent exciting condition is satisfied sometimes. Though sufficient for some applications, they are not well suited for applications which demand not only good output tracking performance but also accurate on-line parameter estimations for secondary purposes such as machine component health monitoring and prognosis. To meet the needs of these applications, in this paper, the integrated direct/indirect adaptive robust control (DIARC) strategy proposed in Yao (2003) will be applied to synthesize coordinated contouring controllers that not only achieve high performance but also possess accurate on-line parameter estimations in implementation.

2. Problem formulation

Since accurate calculation of contouring error often leads to an intensive computation task which is hard to be realized in practice, various approximations have been used in the contouring controls instead. In this paper, the approximation of contouring error in Chen and Lin (2008) and Hu et al. (in press-a) will be used. Specifically, let X and Y, respectively, denote the horizontal and the vertical axes of a biaxial gantry system which also forms a Cartesian coordinate system. At any time instant t, let $\mathbf{q}_d(t) = [x_d(t), y_d(t)]^T$ and $\mathbf{q} = [x(t), y(t)]^T$ be the position vector of the reference trajectory describing the desired contour and the actual position vector of the system in the Cartesian coordinate frame, respectively. Let e_x and e_y be the axial tracking errors of X and Y axes, i.e. $e_x = x - x_d(t)$ and $e_y = y - y_d(t)$, and $\mathbf{e} = [e_x, e_y]^T$ the position tracking error vector in the Cartesian frame. Define a task coordinate frame using the tangential and normal directions of the desired contour at the point $\mathbf{q}_d(t)$ and let $\boldsymbol{\varepsilon} = [\varepsilon_n, \varepsilon_t]^T$ be the position tracking error vector expressed in such a task coordinated frame. Then $\boldsymbol{\varepsilon}$ is related to $\mathbf{e}$ through a unitary transformation matrix $\mathbf{T}$ by

$$\boldsymbol{\varepsilon} = \mathbf{T}\mathbf{e}, \qquad \mathbf{T} = \begin{bmatrix} -\sin\alpha & \cos\alpha \\ \cos\alpha & \sin\alpha \end{bmatrix}, \tag{1}$$

where α denotes the angle between the tangential line of desired contour and the horizontal X-axis. Note that $\mathbf{T}^T = \mathbf{T}$ and $\mathbf{T}^{-1} = \mathbf{T}$ for all values of α. With this definition of task coordinate frame, the actual contouring error $\varepsilon_c(t)$, the shortest distance between the desired contour and the actual contour at the point $\mathbf{q}(t)$, can be approximated reasonably well by ε_n, i.e., $\varepsilon_c \approx \varepsilon_n$, when the axial tracking errors are comparatively small to the curvature of the desired contour. The dynamics of the biaxial linear-motor-driven gantry can be described by (Xu & Yao, 2001a)

$$\mathbf{M}\ddot{\mathbf{q}} + \mathbf{B}\dot{\mathbf{q}} + \mathbf{F}_c(\dot{\mathbf{q}}) = \mathbf{u} + \mathbf{d}, \tag{2}$$

where $\mathbf{M} = \mathrm{diag}[M_1, M_2]$ and $\mathbf{B} = \mathrm{diag}[B_1, B_2]$ are the 2×2 diagonal inertia and viscous friction coefficient matrices, respectively. $\mathbf{F}_c(\dot{\mathbf{q}})$ is the 2×1 vector of Coulomb friction which is modeled by $\mathbf{A}_f\mathbf{S}_f(\dot{\mathbf{q}})$, where $\mathbf{A}_f = \mathrm{diag}[A_{f1}, A_{f2}]$ is the unknown diagonal Coulomb friction coefficient matrix, and $\mathbf{S}_f(\dot{\mathbf{q}}) = [S_f(\dot{x}), S_f(\dot{y})]^T$ is a known vector-valued smooth function used to approximate the traditional discontinuous sign function $sgn(\dot{\mathbf{q}})$ in the traditional Coulomb friction modeling for effective friction compensation in implementation (Xu & Yao, 2001a). $\mathbf{u} = [u_1, u_2]^T$ is the vector of control inputs and $\mathbf{d}$ is the lumped unknown nonlinear functions due to external disturbances and other modeling errors.

Denote $\mathbf{d}_l$ as the lumped modeling errors and disturbances in (2), i.e., $\mathbf{d}_l = \mathbf{d} + \mathbf{A}_f\mathbf{S}_f(\dot{\mathbf{q}}) - \mathbf{F}_c(\dot{\mathbf{q}})$. Let $\mathbf{d}_N = [d_{N1}, d_{N2}]^T$ be the nominal value of $\mathbf{d}_l$ and $\tilde{\mathbf{d}} = \mathbf{d}_l - \mathbf{d}_N$ the time-varying portion of $\mathbf{d}_l$. The system dynamics then become as

$$\mathbf{M}\ddot{\mathbf{e}} + \mathbf{B}\dot{\mathbf{e}} + \mathbf{A}_f\mathbf{S}_f(\dot{\mathbf{q}}) + \mathbf{M}\ddot{\mathbf{q}}_d + \mathbf{B}\dot{\mathbf{q}}_d = \mathbf{u} + \mathbf{d}_l = \mathbf{u} + \mathbf{d}_N + \tilde{\mathbf{d}}. \tag{3}$$

From (1),

$$\dot{\mathbf{e}} = \mathbf{T}\dot{\boldsymbol{\varepsilon}} + \dot{\mathbf{T}}\boldsymbol{\varepsilon}, \qquad \ddot{\mathbf{e}} = \mathbf{T}\ddot{\boldsymbol{\varepsilon}} + 2\dot{\mathbf{T}}\dot{\boldsymbol{\varepsilon}} + \ddot{\mathbf{T}}\boldsymbol{\varepsilon}. \tag{4}$$

The system dynamics in the task coordinate frame can thus be obtained as

$$\begin{aligned}&\mathbf{M}_t\ddot{\boldsymbol{\varepsilon}} + \mathbf{B}_t\dot{\boldsymbol{\varepsilon}} + 2\mathbf{C}_t\dot{\boldsymbol{\varepsilon}} + \mathbf{D}_t\boldsymbol{\varepsilon} + \mathbf{M}_q\ddot{\mathbf{q}}_d + \mathbf{B}_q\dot{\mathbf{q}}_d \\ &\quad + \mathbf{A}_{fq}\mathbf{S}_f(\dot{\mathbf{q}}) = \mathbf{u}_t + \mathbf{d}_t + \tilde{\Delta},\end{aligned} \tag{5}$$

where

$$\begin{aligned}&\mathbf{M}_t = \mathbf{T}\mathbf{M}\mathbf{T}, \mathbf{B}_t = \mathbf{T}\mathbf{B}\mathbf{T}, \mathbf{C}_t = \mathbf{T}\mathbf{M}\dot{\mathbf{T}}, \\ &\mathbf{D}_t = \mathbf{T}\mathbf{M}\ddot{\mathbf{T}} + \mathbf{T}\mathbf{B}\dot{\mathbf{T}}, \mathbf{u}_t = \mathbf{T}\mathbf{u}, \mathbf{d}_t = \mathbf{T}\mathbf{d}_N, \tilde{\Delta} = \mathbf{T}\tilde{\mathbf{d}}, \\ &\mathbf{M}_q = \mathbf{T}\mathbf{M}, \mathbf{B}_q = \mathbf{T}\mathbf{B}, \mathbf{A}_{fq} = \mathbf{T}\mathbf{A}_f.\end{aligned} \tag{6}$$

It is straightforward to verify that the Eq. (5) has the following properties[1] (Yao et al., 1994): (P1) $\mathbf{M}_t$ is a symmetric positive definite (s.p.d.) matrix with $\mu_1\mathbf{I} \le \mathbf{M}_t \le \mu_2\mathbf{I}$ where μ_1 and μ_2 are two positive scalars; (P2) the matrix $\mathbf{N}_t = \dot{\mathbf{M}}_t - 2\mathbf{C}_t$ is a skew-symmetric matrix. In other words, $\mathbf{s}^T\mathbf{N}_t\mathbf{s} = 0, \forall\mathbf{s}$; (P3) $\mathbf{M}_t$, $\mathbf{B}_t$, $\mathbf{C}_t$, $\mathbf{d}_t$, $\mathbf{M}_q$, $\mathbf{B}_q$, $\mathbf{A}_{fq}$ and $\mathbf{d}_t$ in (5) can be linearly parameterized by a set of unknown parameters defined as $\theta = [\theta_1, \ldots, \theta_8]^T = [M_1, M_2, B_1, B_2, A_{f1}, A_{f2}, d_{N1}, d_{N2}]^T$. In general, the parameter vector θ cannot be known exactly. For example, the payload of the biaxial gantry depends on tasks. However, the extent of parametric uncertainties can be predicted and the following practical assumption can be made.

Assumption 1. Extent of parametric uncertainties and uncertain nonlinearities is known. More precisely,

$$\begin{aligned}&\theta \in \Omega_\theta \triangleq \{\theta : \theta_{min} \le \theta \le \theta_{max}\} \\ &\tilde{\Delta} \in \Omega_\Delta \triangleq \left\{\tilde{\Delta} : \|\tilde{\Delta}\| \le \delta_\Delta\right\},\end{aligned} \tag{7}$$

where $\theta_{min} = [\theta_{1min}, \ldots, \theta_{8min}]^T$, and $\theta_{max} = [\theta_{1max}, \ldots, \theta_{8max}]^T$ are known constant vectors and $\boldsymbol{\delta}_\Delta$ is a known function.

3. Direct adaptive robust control (DARC)

In this section, the DARC contouring law in Hu et al. (in press-a, in press-b) is briefly reviewed and will be compared with the proposed DIARC later. Let $\hat{\theta}$ denote the estimate of θ and $\tilde{\theta}$ denote the estimation error (i.e., $\tilde{\theta} = \hat{\theta} - \theta$). In view of (7), the following adaptation law with discontinuous projection modification can be used

$$\dot{\hat{\theta}} = \mathrm{Proj}_{\hat{\theta}}(\Gamma\boldsymbol{\tau}), \tag{8}$$

where $\Gamma > 0$ is a diagonal matrix, $\boldsymbol{\tau}$ is an adaptation function to be synthesized later. The projection mapping $Proj_{\hat{\theta}}(\bullet) = [Proj_{\hat{\theta}_1}(\bullet_1), \ldots, Proj_{\hat{\theta}_8}(\bullet_8)]^T$ is defined as

$$\mathrm{Proj}_{\hat{\theta}_i}(\bullet_i) = \begin{cases} 0 & \text{if } \hat{\theta}_i = \theta_{imax} \text{ and } \bullet_i > 0 \\ 0 & \text{if } \hat{\theta}_i = \theta_{imin} \text{ and } \bullet_i < 0 \\ \bullet_i & \text{otherwise} \end{cases} \tag{9}$$

which has the following properties (Yao & Tomizuka, 1996)

$$\begin{aligned}&(\text{P4})\, \hat{\theta} \in \Omega_\theta \triangleq \left\{\hat{\theta} : \theta_{min} \le \hat{\theta} \le \theta_{max}\right\} \\ &(\text{P5})\, \tilde{\theta}^T(\Gamma^{-1}\mathrm{Proj}_{\hat{\theta}}(\Gamma\boldsymbol{\tau}) - \boldsymbol{\tau}) \le 0, \quad \forall\boldsymbol{\tau}.\end{aligned} \tag{10}$$

[1] The following nomenclature is used throughout this paper: $\bullet_{min}$ and $\bullet_{max}$ are the minimum value and maximum value of $\bullet$ respectively, $\hat{\bullet}$ denotes the estimate of $\bullet$, $\tilde{\bullet} = \hat{\bullet} - \bullet$ denotes the estimation error, e.g., $\tilde{\theta} = \hat{\theta} - \theta$, $\bullet_i$ is the ith component of the vector $\bullet$, and the operation $\le$ for two vectors is performed in terms of the corresponding elements of the vectors.

Define a switching-function-like quantity and a positive semi-definite (p.s.d.) function as

$$\mathbf{s} = \dot{\boldsymbol{\varepsilon}} + \Lambda \boldsymbol{\varepsilon}, \qquad V(t) = \frac{1}{2}\mathbf{s}^T \mathbf{M}_t \mathbf{s}, \tag{11}$$

where $\Lambda > 0$ is a diagonal matrix. From (5),

$$\begin{aligned}\dot{V} &= \mathbf{s}^T \Big[\mathbf{u}_t + \mathbf{d}_t + \widetilde{\Delta} - \mathbf{M}_q \ddot{\mathbf{q}}_d - \mathbf{B}_q \dot{\mathbf{q}}_d - \mathbf{A}_{fq}\mathbf{S}_f(\dot{\mathbf{q}}) \\ &\quad - \mathbf{B}_t \dot{\boldsymbol{\varepsilon}} - \mathbf{C}_t \dot{\boldsymbol{\varepsilon}} - \mathbf{D}_t \boldsymbol{\varepsilon} + \mathbf{C}_t \Lambda \boldsymbol{\varepsilon} + \mathbf{M}_t \Lambda \dot{\boldsymbol{\varepsilon}}\Big] \\ &= \mathbf{s}^T[\mathbf{u}_t + \Psi(\mathbf{q}, \dot{\mathbf{q}}, t)\theta + \widetilde{\Delta}],\end{aligned} \tag{12}$$

where (P2) is used to eliminate the term $\frac{1}{2}\mathbf{s}^T \dot{\mathbf{M}}_t \mathbf{s}$ in the derivation of the first equation and (P3) to obtain the expression of 2×8 matrix $\Psi(\mathbf{q}, \dot{\mathbf{q}}, t)$ of known functions, commonly referred to as the regressor. The DARC law in Hu et al. (in press-a) has the structure of

$$\mathbf{u}_t = \mathbf{u}_a + \mathbf{u}_s, \quad \mathbf{u}_a = -\Psi(\mathbf{q}, \dot{\mathbf{q}}, t)\widehat{\theta}, \tag{13}$$

where $\mathbf{u}_a$ is the adjustable model compensation needed to achieve perfect output tracking and $\mathbf{u}_s$ is a robust control law consisting of two terms:

$$\mathbf{u}_s = \mathbf{u}_{s1} + \mathbf{u}_{s2}, \quad \mathbf{u}_{s1} = -\mathbf{K}\mathbf{s} \tag{14}$$

in which $\mathbf{u}_{s1}$ is a simple proportional feedback to stabilize the nominal system with $\mathbf{K}$ being a symmetric positive definite matrix for simplicity, and $\mathbf{u}_{s2}$ is a feedback used to attenuate the effect of model uncertainties to a certain level for a guaranteed robust performance. Specifically, noting Assumption 1 and (P4), there exists a $\mathbf{u}_{s2}$ such that the following two robust performance conditions are satisfied (Yao, 1997; Yao & Tomizuka, 2001):

$$\begin{aligned}&\text{i.} \quad \mathbf{s}^T[\mathbf{u}_{s2} - \Psi(\mathbf{q}, \dot{\mathbf{q}}, t)\widetilde{\theta} + \widetilde{\Delta}] \le \eta \\ &\text{ii.} \quad \mathbf{s}^T \mathbf{u}_{s2} \le 0,\end{aligned} \tag{15}$$

where η is a design parameter quantifying the level of uncertainties attenuation.

4. Integrated direct/indirect adaptive robust control (DIARC)

In this section, the DIARC control strategy in Yao (2003) is applied to synthesize a contouring control law for the system (5). As in DARC in the previous section, the first step is to use a projection-type adaptation law structure to achieve a controlled learning or adaptation process. But unlike DARC designs, the least-squares-type adaptation law will be used to achieve better convergence of parameter estimations and the adaptation rate matrix will be time-varying and non-diagonal. As such, the simple discontinuous projection mapping (9) used in DARC designs cannot be used theoretically since such a discontinuous projection mapping is valid only for diagonal adaptation rate matrix Γ. Instead, the following standard projection mapping in adaptive control (Goodwin & Mayne, 1987) should be used to keep the parameter estimates within the known bounded set $\overline{\Omega}_\theta$, the closure of the set Ω_θ:

$$\mathrm{Proj}_{\widehat{\theta}}(\zeta) = \begin{cases} \zeta, & \text{if } \widehat{\theta} \in \mathring{\Omega}_\theta \text{ or } \left(\widehat{\theta} \in \partial\Omega_\theta \text{ and } n_{\widehat{\theta}}^T \zeta \le 0\right) \\ \left(I - \Gamma \dfrac{n_{\widehat{\theta}} n_{\widehat{\theta}}^T}{n_{\widehat{\theta}}^T \Gamma n_{\widehat{\theta}}}\right)\zeta, & \text{if } \widehat{\theta} \in \partial\Omega_\theta \text{ and } n_{\widehat{\theta}}^T \zeta > 0 \end{cases} \tag{16}$$

where $\zeta \in R^p$ is any function and $\Gamma(t) \in R^{p \times p}$ can be any time-varying positive definite symmetric matrix. In (16), $\mathring{\Omega}_\theta$ and $\partial\Omega_\theta$ denote the interior and the boundary of Ω_θ respectively, and $n_{\widehat{\theta}}$ represents the outward unit normal vector at $\widehat{\theta} \in \partial\Omega_\theta$. It can be verified that the projection-type adaptation law (8) with such a projection still has the (P4) and (P5) in (10) (Yao & Tomizuka, 1996).

4.1. Integrated DIARC contouring control law synthesis

Through use of the projection-type adaptation law, parameter estimates are bounded with known bounds, regardless of the estimation function τ to be used. This property will be used in this subsection to synthesize an integrated DIARC contouring control law that achieves a guaranteed transient performance and steady-state contouring accuracy regardless how the physical parameters will be estimated. Specifically, the proposed DIARC control law has the following form:

$$\begin{aligned}&\mathbf{u}_t = \mathbf{u}_a + \mathbf{u}_s, \quad \mathbf{u}_a = \mathbf{u}_{a1} + \mathbf{u}_{a2}, \ \mathbf{u}_s = \mathbf{u}_{s1} + \mathbf{u}_{s2}, \\ &\mathbf{u}_{a1} = -\Psi(\mathbf{q}, \dot{\mathbf{q}}, t)\widehat{\theta}, \qquad \mathbf{u}_{s1} = -\mathbf{K}\mathbf{s},\end{aligned} \tag{17}$$

where $\mathbf{u}_{a1}$ is the adjustable model compensation needed for perfect tracking with $\widehat{\theta}$ being the on-line estimates of physical parameters to be detailed later, $\mathbf{u}_{a2}$ is a fast dynamic compensation term synthesized below, and $\mathbf{u}_{s1}$ and $\mathbf{u}_{s2}$ have the same meanings as in DARC designs. For V given by (11), substituting (17) into (12) and simplifying the resulting expression lead to

$$\dot{V} = \mathbf{s}^T[\mathbf{u}_{a2} + \mathbf{u}_s - \Psi(\mathbf{q}, \dot{\mathbf{q}}, t)\widetilde{\theta} + \widetilde{\Delta}]. \tag{18}$$

Define a constant $\mathbf{d}_c$ and time varying function $\widetilde{\mathbf{d}}^*(t)$ such that

$$\mathbf{T}\mathbf{d}_c + \widetilde{\mathbf{d}}^*(t) = -\Psi(\mathbf{q}, \dot{\mathbf{q}}, t)\widetilde{\theta} + \widetilde{\Delta}. \tag{19}$$

Conceptually, (19) lumps the disturbance and the model uncertainties due to parameter estimation error together and divides it into the low frequency component $\mathbf{d}_c$ and the higher frequency components $\widetilde{\mathbf{d}}^*(t)$, so that the low frequency component $\mathbf{d}_c$ can be compensated through the fast dynamic compensation-type adaptation as in the previous DARC design as follows. Substituting (19) into (18),

$$\dot{V} = \mathbf{s}^T[\mathbf{u}_{a2} + \mathbf{u}_s + \mathbf{T}\mathbf{d}_c + \widetilde{\mathbf{d}}^*(t)]. \tag{20}$$

Choose the fast dynamic compensation term $\mathbf{u}_{a2}$ as

$$\mathbf{u}_{a2} = -\mathbf{T}\widehat{\mathbf{d}}_c, \tag{21}$$

where $\widehat{\mathbf{d}}_c$ represents the estimate of $\mathbf{d}_c$ updated by

$$\dot{\widehat{\mathbf{d}}}_c = \mathrm{Proj}_{\widehat{\mathbf{d}}_c}(\gamma_d \mathbf{T}\mathbf{s}), \qquad |\widehat{\mathbf{d}}_c(0)| \le \widehat{\mathbf{d}}_{cmax}, \tag{22}$$

in which $\widehat{\mathbf{d}}_{cmax}$ is a pre-set bound for $\widehat{\mathbf{d}}_c(t)$ and $\gamma_{\mathbf{d}}$ is a 2×2 constant diagonal matrix. As in DARC designs in Section 3, the projection mapping in (22) guarantees that $|\widehat{\mathbf{d}}_c(t)| \le \widehat{\mathbf{d}}_{cmax}$, $\forall t$. Thus, similar to (15), one can choose a robust feedback term $\mathbf{u}_{s2}$ to meet the following two conditions for a guaranteed robust performance:

$$\begin{aligned}&\text{i.} \quad \mathbf{s}^T[\mathbf{u}_{s2} - \mathbf{T}\widetilde{\mathbf{d}}_c + \widetilde{\mathbf{d}}^*(t)] \le \eta \\ &\text{ii.} \quad \mathbf{s}^T \mathbf{u}_{s2} \le 0,\end{aligned} \tag{23}$$

where $\widetilde{\mathbf{d}}_c = \widehat{\mathbf{d}}_c - \mathbf{d}_c$ and η is a design parameter quantifying the level of attenuation to be achieved. For example, one smooth example of $\mathbf{u}_{s2}$ satisfying (23) is given by $\mathbf{u}_{s2} = -\frac{1}{4\eta}h^2\mathbf{s}$, where h is any smooth function satisfying $h \ge \|\widehat{\mathbf{d}}_{cmax}\| + \|\theta_{\mathbf{M}}\|\|\Psi(\mathbf{q}, \dot{\mathbf{q}}, t)\| + \delta_\Delta$, and $\theta_{\mathbf{M}} = \theta_{max} - \theta_{min}$ (Yao, 2003).

Theorem 1. *Consider the DIARC control law (17) in which the physical parameter estimates $\widehat{\theta}$ are updated by the projection-type adaptation law (8) with projection (16) and the dynamic compensation $\widehat{\mathbf{d}}_c$ is updated by (22) with projection (9). Regardless the estimation function τ to be used, in general, all signals in the resulting closed loop system are bounded and the contouring error and output position tracking error are guaranteed to have a prescribed transient performance and steady-state accuracy in the sense that $V(t)$ defined by (11) is bounded by*

$$V(t) \le \exp(-\lambda t)V(0) + \frac{\eta}{\lambda}[1 - \exp(-\lambda t)], \tag{24}$$

where $\lambda = 2\sigma_{min}(\mathbf{K})/\mu_2$ in which $\sigma_{min}(\cdot)$ denotes the minimum singular value of a matrix and μ_2 is defined in property (P1).

4.2. Estimation of physical parameters

Regardless of the estimation function τ to be used, the above DIARC control law achieves a guaranteed transient and steady-state performance even in the presence of uncertain nonlinearities. Thus, this subsection focuses on the construction of suitable estimation functions τ so that an improved steady-state performance—asymptotic output tracking or zero steady-state contouring and position tracking error—can be obtained even when all physical parameters are unknown. In addition, it is desirable to have on-line parameter estimates converge or stay close to their true values so that they can be used for other purposes such as machine component health monitoring. To this end, in this subsection, it is assumed that the system has parametric uncertainties only, i.e., assuming $\widetilde{\mathbf{d}} = 0$ in (5). To avoid the need of acceleration feedback in the following estimation of physical parameters, let $H_f(s)$ be the transfer function of any filter with a relative degree larger than or equal to 1 (e.g., $H_f(s) = 1/(\tau_f s + 1)$) and apply the filter to both sides of (3) to obtain the parameter estimation model as follows. When $\widetilde{\mathbf{d}} = 0$, one obtains

$$\mathbf{u}_f = \Upsilon_f^T \theta, \quad \mathbf{u}_f = \begin{bmatrix} u_{1f} \\ u_{2f} \end{bmatrix}, \quad \Upsilon_f^T = \begin{bmatrix} \ddot{x}_f, 0, \dot{x}_f, 0, S_{ff}(\dot{x}), 0, -1_f, 0 \\ 0, \ddot{y}_f, 0, \dot{y}_f, 0, S_{ff}(\dot{y}), 0, -1_f \end{bmatrix}, \tag{25}$$

in which $\bullet_f$ represents the filtered value of $\bullet$. Define the prediction error vector as $\boldsymbol{\varsigma} = \widehat{\mathbf{u}}_f - \mathbf{u}_f$ where $\widehat{\mathbf{u}}_f = \Upsilon_f^T \widehat{\theta}$. Then the prediction error vector $\boldsymbol{\varsigma}$ is related to the parameter estimation error as

$$\boldsymbol{\varsigma} = \Upsilon_f^T \widehat{\theta} - \mathbf{u}_f = \Upsilon_f^T \widetilde{\theta} \tag{26}$$

which is in the standard linear regression model form. Thus, various well-known parameter estimation algorithms can be used to obtain the estimates of θ. For example, when the least-squares-type estimation algorithm with co-variance limiting is used, $\hat{\theta}$ is updated by the adaptation law (8) with the adaptation function given by (Yao, 2003)

$$\tau = -\frac{1}{1 + \upsilon tr\{\Upsilon_f^T \Gamma \Upsilon_f\}} \Upsilon_f \varsigma \tag{27}$$

and the adaptation rate matrix given by

$$\dot{\Gamma} = \begin{cases} \kappa \Gamma - \dfrac{1}{1 + \upsilon tr\{\Upsilon_f^T \Gamma \Upsilon_f\}} \Gamma \Upsilon_f \Upsilon_f^T \Gamma, & \text{if } \lambda_{max}(\Gamma) \leq \rho_M \\ 0, & \text{otherwise} \end{cases} \tag{28}$$

where $\kappa \geq 0$ is the forgetting factor, ρ_M is the pre-set upper bound for $\|\Gamma(t)\|$, $\upsilon \geq 0$ with $\upsilon = 0$ leading to the unnormalized algorithm. With these practical modifications, $\Gamma(t) \leq \rho_M I, \ \forall t$. The following theorem summarize the improved performance of the proposed DIARC (Yao, 2003):

Theorem 2. *Consider the situation where only parametric uncertainties exist after a finite time t_0, i.e., $\widetilde{\mathbf{d}} = 0, \forall t \geq t_0$ in (5). Then, when the DIARC control law (17) and the projection-type adaption law (8) are used with the least-squares-type estimation function (27), in addition to the robust performance results stated in Theorem 1, an improved steady-state contouring performance – asymptotic contouring tracking (i.e., $\boldsymbol{\varepsilon} \to 0$ and $\mathbf{s} \to 0$ as $t \to \infty$) – is also achieved along with the convergence of physical parameter estimates to their true values when the following PE condition (29) is satisfied: there exist $\kappa_p > 0$ and $T > 0$ such that*

$$\int_t^{t+T} \Upsilon_f \Upsilon_f^T \mathrm{d}\tau \geq \kappa_p I_p, \quad \forall t. \tag{29}$$

5. Experimental setup and results

A biaxial Anorad HERC-510-510-AA1-B-CC2 gantry from Rockwell Automation has been set up in Zhejiang University as a test-bed for contouring control problems. As shown in Fig. 1, the two axes powered by Anorad LC-50-200 iron core linear motors are mounted orthogonally with X-axis on top of Y-axis. The position sensors of the gantry are two linear encoders with a resolution of 0.5 μm after quadrature. The velocity signal is obtained by the difference of two consecutive position measurements. Standard least-square identification is performed to obtain the parameters of the biaxial gantry and it is found that nominal values of the gantry system parameters without loads are $M_1 = 0.12(\mathrm{V/m/s^2})$, $M_2 = 0.5(\mathrm{V/m/s^2})$, $B_1 = 0.5(\mathrm{V/m/s})$, $B_2 = 0.7(\mathrm{V/m/s})$, $A_{f1} = 0.1(\mathrm{V})$, $A_{f2} = 0.15(\mathrm{V})$, $d_{N1} = 0$, $d_{N2} = 0$; these values are a little different from those in Hu et al. (in press-a, in press-b) because some lubricant has been added to the bearings of both axes for preventive maintenance since then. In addition, through direct measurement of input voltages and the resulting forces when the motor is blocked, the gain from the input voltage to the force applied to the load is found to be $k_f = 69$ N/V. The bounds of the parametric variations are chosen as $\theta_{min} = [0.05, 0.45, 0.35, 0.5, 0.05, 0.08, -0.5, -1]^T$ and $\theta_{max} = [0.20, 0.6, 0.55, 0.8, 0.15, 0.25, 0.5, 1]^T$, which cover the entire range of various loading conditions of the system. The following performance indexes will be used to quantify the quality of each control algorithm: (i) $\|\varepsilon_c\|_{rms} = (\frac{1}{T}\int_0^T |\varepsilon_c|^2 \mathrm{d}t)^{1/2}$, the root-mean-square (RMS) value of the contouring error where T is the duration of the time period interested; (ii) $\varepsilon_{cM} = \max_t \{|\varepsilon_c|\}$, the maximum absolute value of the contouring error during the time period of interest; and (iii) $\widehat{\theta}_{iv} = \max\{|\frac{\widehat{\theta}_{ic} - \theta_{iN}}{\theta_{iN}}|, |\frac{\widehat{\theta}_{ie} - \theta_{iN}}{\theta_{iN}}|\}$, the maximum percentage variations of on-line steady-state parameter estimates to their off-line estimated values, as measures of the accuracy of parameter estimations, in which $\widehat{\theta}_{ic}$ and $\widehat{\theta}_{ie}$ are the steady-state value of the ith parameter estimate in circular contouring experiment and in elliptical contouring experiment respectively, and θ_{iN} the off-line estimated value of θ_i.

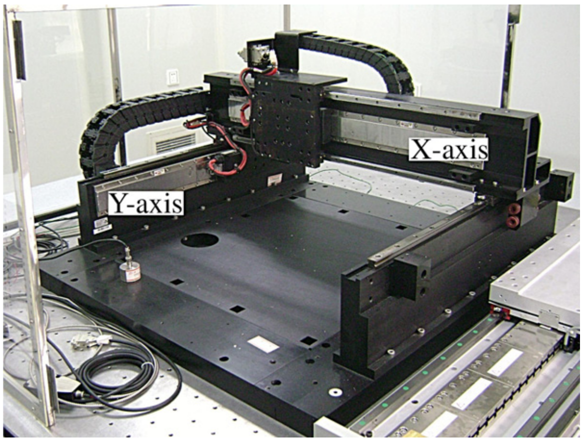

Fig. 1. A Biaxial linear motor driven gantry system.

The control algorithms are implemented using a dSPACE DS1103 controller board executing programs at a sampling period of $T_s = 0.2$ ms, resulting in a velocity measurement resolution of 0.0025 m/s. The following three control algorithms are compared:

C1: direct adaptive robust control (DARC)—the control law presented in Section 3.
C2: integrated direct/indirect adaptive robust control (DIARC)—the proposed control law in Section 4.
C3: deterministic robust control (DRC)—the DARC control law without using on-line adaptation (i.e., set $\Gamma = 0\mathbf{I}_8$ in C1).

For a fair comparison, the controller parameter values of all controllers are chosen the same if they have the same physical meanings. Specifically, for all controllers, $S_f(\dot{x})$ and $S_f(\dot{y})$ are

Table 1
Circular contouring results (The first row below the controllers are for $\|\varepsilon_c\|_{rms}$ in μm and the second row for ε_{cM} in μm).

Set 1			Set 2			Set 3	
C1	C2	C3	C1	C2	C3	C1	C2
2.03	1.99	7.33	2.18	2.02	8.36	2.36	2.30
7.31	7.14	21.0	8.16	6.85	19.78	26.81	28.43

chosen as $\frac{2}{\pi}\arctan(9000\dot{x})$ and $\frac{2}{\pi}\arctan(9000\dot{y})$ respectively, and $\Lambda = \mathrm{diag}[100, 30]$. Mathematically, one should use the form of $\mathbf{u}_{s2} = -\mathbf{K}_{s2}(\mathbf{q}, \dot{\mathbf{q}}, t)\mathbf{s}$ with $\mathbf{K}_{s2}$ being a nonlinear proportional feedback gain (e.g., $\mathbf{K}_{s2} = \frac{1}{4\eta}h^2$ for the specific example given below Eq. (23) so that robust performance conditions like (23) can be satisfied globally. In implementation, a large enough constant feedback gain $\mathbf{K}_{s2}$ can be used instead to simplify the resulting control law. With such a simplification, though the robust performance condition (23) may not be guaranteed globally, the condition can still be satisfied in a large enough working range which might be acceptable to practical applications as done in Yao, Bu, Reedy, and Chiu (2000). With this simplification, noting (17), we choose $\mathbf{u}_s = -\mathbf{K}_s\mathbf{s}$ in the experiments where $\mathbf{K}_s$ represents the combined gain of $\mathbf{K}$ and $\mathbf{K}_{s2}$; the specific values used in both controllers are $\mathbf{K}_s = \mathrm{diag}[100, 60]$. The adaptation rates in C1 are set as $\Gamma = \mathrm{diag}[10, 10, 10, 10, 1, 1, 10\,000, 10\,000]$ with initial parameter estimates chosen to be $\hat{\theta}(0) = [0.1, 0.55, 0.35, 0.5, 0.1, 0.15, 0, 0]^T$ for all experiments. The bounds of $\hat{\mathbf{d}}_c$ in (22) is set as $\hat{\mathbf{d}}_{cmax} = [0.5, 1.5]^T$ with $\gamma_{\mathbf{d}} = \mathrm{diag}[10\,000, 10\,000]$. Second-order transfer functions of damping ratio of 0.7 and natural frequencies of 250 Hz for X-axis and 150 Hz for Y-axis are used for the filters in Section 4.2. In (28), a forgetting factor of $\kappa = 0.1$ and a normalization value of $\upsilon = 0.1$ are used. The initial adaptation rates are set as $\Gamma(0) = \mathrm{diag}[10, 10, 10, 10, 10, 10, 5000, 5000]$ and $\rho_M = 500$ and the same initial parameter estimates as in C1 are used in C2. The following test sets are performed.

Set 1: Experiments are run without payload, which is equivalent to $M_1 = 0.12$ and $M_2 = 0.5$.
Set 2: A 5 kg payload is mounted on the gantry, which is equivalent to $M_1 = 0.19$ and $M_2 = 0.57$.
Set 3: A step disturbance (a simulated 0.6 V electrical signal) is added to the input of Y axis at $t = 1.86$ s and removed at $t = 4.86$ s to test the performance robustness of each controller to input disturbances.

5.1. *Circular contouring with constant velocity*

The biaxial gantry is first commanded to track a circle having a radius of 0.2 m and a desired velocity of $\upsilon = 0.4$ m/s on the contour. The circular contouring experimental results in terms of performance indexes after running the gantry for one period are given in Table 1. Overall, both DARC and DIARC achieve good steady-state contouring performance during fast circular movements. Specifically, for both Set 1 and Set 2, the contouring errors of DARC and DIARC are mostly within 5 μm and roughly one-third of those in DRC, demonstrating the significantly improved performance of using on-line adaptation and the performance robustness of the proposed controllers to parameter variations. The contouring errors of Set 3 for DARC and DIARC are given in Fig. 2. As seen from the figures, the added disturbances do not affect the contouring performance much except the transient spikes when the step disturbances occur. These results demonstrate the strong performance robustness of the proposed algorithms to disturbances as well.

5.2. *Elliptical contouring with constant angular velocity*

To test the contouring performance of the proposed algorithms for non-circular motions, the biaxial gantry is also commanded

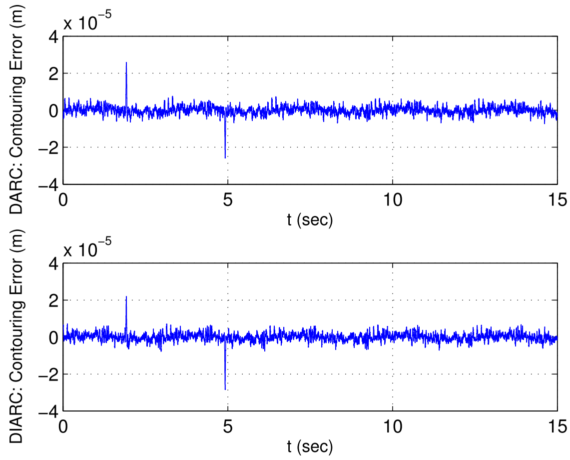

Fig. 2. Circular contouring errors of Set3 (disturbances).

Table 2
Elliptical contouring results (the first row below the controllers are for $\|\varepsilon_c\|_{rms}$ in μm and the second row for ε_{cM} in μm).

Set 1			Set 2			Set 3	
C1	C2	C3	C1	C2	C3	C1	C2
2.63	2.61	7.00	2.89	2.66	11.4	3.10	2.91
9.35	8.19	18.17	10.31	8.96	30.1	25.4	26.0

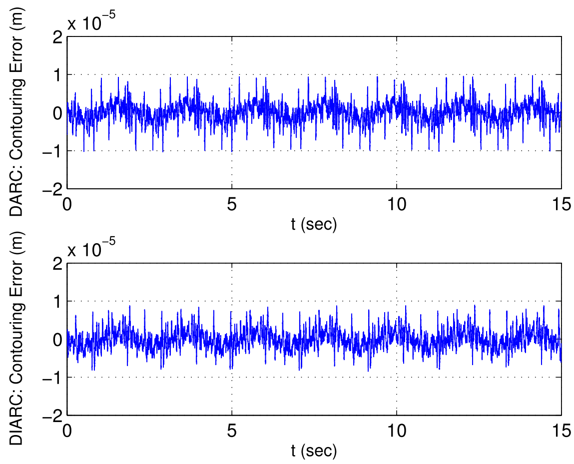

Fig. 3. Elliptical contouring errors of Set2 (loaded).

to track an ellipse described by $\mathbf{q}_d = [0.2\sin(3t), \ -0.1\cos(3t) + 0.1]^T$ which has a time-varying contouring velocity of $0.3\sqrt{1 + 3\cos^2(3t)}$ m/s though a constant angular velocity of $\omega = 3$ rad/s. The elliptical contouring experimental results in terms of performance indexes after running the gantry for one period are given in Table 2. Again, both DARC and DIARC achieve good steady-state contouring performance during the fast elliptical movements. For Set 1, the contouring errors of DARC and DIARC are mostly within 5 μm as well, significantly less than in DRC, demonstrating the need of using on-line adaptation. For Set 2, the contouring errors are shown in Fig. 3, revealing almost the same level of steady-state contouring performance as without the payload. This again demonstrates the strong performance robustness of the proposed contouring controllers to parameter variations. Though not shown due to the page limit, the contouring errors of Set 3 are similar to those in circular experiments. All these results further demonstrate the strong performance robustness of the proposed schemes to disturbances.

Table 3
Physical parameter estimations of DIARC without load.

	M_1	M_2	B_1	B_2	A_{f1}	A_{f2}
θ_{iN}	0.12	0.5	0.5	0.7	0.1	0.15
$\widehat{\theta}_{ic}$	0.111	0.483	0.522	0.730	0.102	0.150
$\widehat{\theta}_{ie}$	0.115	0.505	0.464	0.670	0.104	0.147
$\widehat{\theta}_{iv}$	7.5%	3.4%	7.2%	4.3%	4.0%	2.0%

Table 4
Physical parameter estimations of DIARC with 5 kg load.

	M_1	M_2	B_1	B_2	A_{f1}	A_{f2}
θ_{iN}	0.19	0.57	0.5	0.7	0.1	0.15
$\widehat{\theta}_{ic}$	0.182	0.562	0.500	0.642	0.102	0.163
$\widehat{\theta}_{ie}$	0.188	0.578	0.462	0.720	0.105	0.15
$\widehat{\theta}_{iv}$	4.2%	1.4%	7.6%	8.3%	5.0%	8.7%

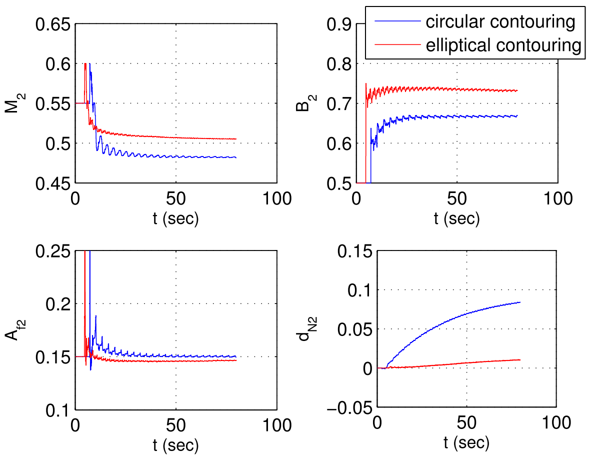

Fig. 4. Y-axis parameter estimates of Set1 (no load).

5.3. Parameter estimation results

Though both DARC and DIARC achieve excellent contouring performance, unlike DARC, the proposed DIARC has good on-line parameter estimations as well. To see this, the steady-state values of the parameter estimates of the proposed DIARC during both the circular and elliptical contouring motions are given in Table 3 for no-load experiments and in Table 4 for loaded experiments respectively. Typical histories of on-line parameter estimates can be seen from Fig. 4, the parameter estimates of Y-axis during no-load experiments, and from 5, the parameter estimates of X-axis during loaded experiments. As shown, on-line estimates of physical parameters all converge and stay close to their off-line estimated values with maximum estimation errors less than 9% in all cases, which might be accurate enough for them to be used for other purposes such as the component health monitoring. All these results demonstrate the potential accurate on-line parameter estimation capability of the proposed DIARC contouring controller in implementation.

6. Conclusions

In this paper, an integrated DIARC contouring controller that possesses not only excellent contouring performance but also accurate parameter estimations is developed and tested on a biaxial linear-motor-driven industrial gantry system. The unique feature of the proposed DIARC contouring controller is that the parameter estimation process is completely independent of the control law design, allowing the use of estimation algorithms having better convergence properties such as the least-squares type and the explicit on-line monitoring of signal excitation levels for accurate parameter estimations. In addition, dynamic compensation-type fast adaptations similar to those in DARC designs are also introduced to preserve the excellent contouring performance of DARC designs. Comparative experimental results verify the excellent contouring performance and the accurate estimations of physical parameters of the proposed DIARC contouring controller in practice.

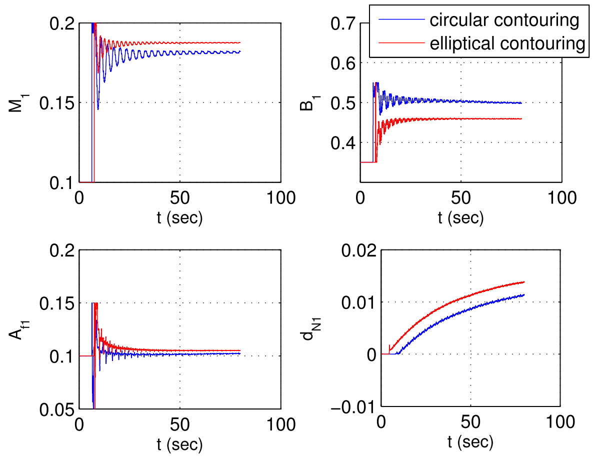

Fig. 5. X-axis parameter estimates of Set2 (loaded).

Appendix

Proof of Theorem 1. Substituting (21) into (20) and noting i of (23),

$$\dot{V} = \mathbf{s}^T[-\mathbf{K}\mathbf{s} + \mathbf{u}_{s2} - \mathbf{T}\widetilde{\mathbf{d}}_c + \widetilde{\mathbf{d}}^*(t)] \leq -\mathbf{s}^T\mathbf{K}\mathbf{s} + \eta$$
$$\leq -\lambda V + \eta \quad (30)$$

which leads to (24) by the comparison lemma. The rest of Theorem 1 can thus be verified easily. ∎

Proof of Theorem 2. Choose a positive function as

$$V_a = V + \frac{1}{2}\widetilde{\mathbf{d}}_c^T \gamma_{\mathbf{d}}^{-1}\widetilde{\mathbf{d}}_c \quad (31)$$

where V is given by (11). Noting the assumption that $\widetilde{\Delta} = 0$, from (18) and (21),

$$\dot{V}_a = \mathbf{s}^T[-\mathbf{T}\widehat{\mathbf{d}}_c + \mathbf{u}_s - \Psi(\mathbf{q}, \dot{\mathbf{q}}, t)\widetilde{\theta}] + \widetilde{\mathbf{d}}_c^T \gamma_{\mathbf{d}}^{-1}\dot{\widehat{\mathbf{d}}}_c$$
$$= -\mathbf{s}^T\mathbf{K}\mathbf{s} + \mathbf{s}^T\mathbf{u}_{s2} - \mathbf{s}^T\Psi(\mathbf{q}, \dot{\mathbf{q}}, t)\widetilde{\theta} + \widetilde{\mathbf{d}}_c^T[\gamma_{\mathbf{d}}^{-1}\dot{\widehat{\mathbf{d}}}_c - \mathbf{T}\mathbf{s}]. \quad (32)$$

Noting (22) and ii of (23),

$$\dot{V}_a \leq -\mathbf{s}^T\mathbf{K}\mathbf{s} - \mathbf{s}^T\Psi(\mathbf{q}, \dot{\mathbf{q}}, t)\widetilde{\theta} + \widetilde{\mathbf{d}}_c^T\left[\gamma_{\mathbf{d}}^{-1}\mathrm{Proj}_{\widehat{\mathbf{d}}_c}(\gamma_d\mathbf{T}\mathbf{s}) - \mathbf{T}\mathbf{s}\right]$$
$$\leq -\mathbf{s}^T\mathbf{K}\mathbf{s} - \mathbf{s}^T\Psi(\mathbf{q}, \dot{\mathbf{q}}, t)\widetilde{\theta} \quad (33)$$

in which the projection property (P5) is used by treating $\mathbf{d}_c = 0$. When the PE condition (29) is satisfied, it can be shown that the standard estimation algorithm leads to the convergence of parameter estimates to their true values and $\widetilde{\theta} \in L_2[0, \infty)$. Since $\Psi(\mathbf{q}, \dot{\mathbf{q}}, t)$ is bounded due to Theorem 1, $\Psi(\mathbf{q}, \dot{\mathbf{q}}, t)\widetilde{\theta} \in L_2[0, \infty)$ as well. From (33), $\mathbf{s} \in L_2[0, \infty)$. By Barbalat's Lemma, asymptotic contouring tracking can be proved. ∎

References

Cheng, M.-. Y., & Lee, C.-. C. (2007). Motion controller design for contour-following tasks based on real-time contour error estimation. *IEEE Transactions on Industrial Electronics*, *54*(3), 1686–1695.

Chen, C.-L., & Lin, K.-C. (2008). Observer-based contouring controller design of a biaxial stage system subject to friction. *IEEE Transactions on Control System Technology*, *16*(2), 322–329.

Chiu, G. T. C., & Tomizuka, M. (2001). Contouring control of machine tool feed drive systems: a task coordinate frame approach. *IEEE Transactions on Control Systems Technology*, *9*(Jan.), 130–139.

Chiu, T. C., & Yao, B. (1997). Adaptive robust contour tracking of machine tool feed drive systems - A task coordinate frame approach. In *Proc. of American Control Conference (Vol. 5)* (pp. 2731–2735).

Goodwin, G. C., & Mayne, D. Q. (1987). A parameter estimation perspective of continuous time model reference adaptive control. *Automatica*, *23*(1), 57–70.

Hong, Y., & Yao, B. (2007). A globally stable saturated desired compensation adaptive robust control for linear motor systems with comparative experiments. *Automatica*, *43*(10), 1840–1848.

Hu, C., Yao, B., & Wang, Q. (2009a). Coordinated adaptive robust contouring controller design for an industrial biaxial precision gantry. IEEE/ASME Transactions on Mechatronics. in press (doi:10.1109/TMECH.2009.2032292). Part of the paper was presented in *2009 IEEE/ASME conference on advanced intelligent mechatronics* (pp. 1810–1815), Singapore, July 2009.

Hu, C., Yao, B., & Wang, Q. (2009b). Coordinated adaptive robust contouring control of an industrial biaxial precision gantry with cogging force compensations. IEEE Transactions on Industrial Electronics, in press (doi:10.1109/TIE.2009.2030769).

Koren, Y. (1980). Cross-coupled biaxial computer control for manufacturing systems. *ASME Journal of Dynamical Systems, Measurement, and Control*, *102*, 265–272.

Li, P. Y. (1999). Coordinated contour following control for machining operations — A survey. In *Amer. control conf.* (pp. 4543–4547).

Lu, L., Chen, Z., Yao, B., & Wang, Q. (2008). Desired compensation adaptive robust control of a linear motor driven precision industrial gantry with improved cogging force compensation. *IEEE/ASME Transactions on Mechatronics*, *13*(6), 617–624.

Lu, L., Yao, B., Wang, Q., & Chen, Z. (2009). Adaptive robust control of linear motors with dynamic friction compensation using modified lugre model. *Automatica*, *45*(12), 2890–2896.

Xu, L., & Yao, B. (2008). Adaptive robust control of mechanical systems with nonlinear dynamic friction compensation. *International Journal of Control*, *81*(2), 167–176.

Xu, L., & Yao, B. (2000). Coordinated adaptive robust contour tracking of linear-motor-driven tables in task space. In *Proc. of IEEE conf. on decision and control*. Sydney (pp. 2430–2435).

Xu, L., & Yao, B. (2001a). Adaptive robust precision motion control of linear motors with negligible electrical dynamics: Theory and experiments. *IEEE/ASME Transactions on Mechatronics*, *6*(4), 444–452.

Xu, L., & Yao, B. (2001b). Output feedback adaptive robust precision motion control of linear motors. *Automatica*, *37*(7), 1029–1039.

Yao, B. (1997). High performance adaptive robust control of nonlinear systems: a general framework and new schemes. In *Proc. of IEEE conference on decision and control*, San Diego (pp. 2489–2494).

Yao, B. (1998). Desired compensation adaptive robust control. In *The ASME International Mechanical Engineers Congress and Exposition (IMECE). DSC-Vol. 64*, pp. 569–575. Anaheim. Revised full paper will appear in Transactions of ASME, Journal of Dynamic Systems, Measurement and Control, 2009.

Yao, B. (2003). Integrated direct/indirect adaptive robust control of SISO nonlinear systems transformable to semi-strict feedback forms. In *American Control Conference* (pp. 3020–3025). The O. Hugo Schuck Best Paper (Theory) Award from the American Automatic Control Council in 2004.

Yao, B., Bu, F., Reedy, J., & Chiu, G. T. C. (2000). Adaptive robust control of single-rod hydraulic actuators: Theory and experiments. *IEEE/ASME Transactions on Mechatronics*, *5*(1), 79–91.

Yao, B., Chan, S. P., & Wang, D. (1994). Unified formulation of variable structure control schemes to robot manipulators. *IEEE Transactions on Automatic Control*, *39*(2), 371–376.

Yao, B., & Tomizuka, M. (1996). Smooth robust adaptive sliding mode control of robot manipulators with guaranteed transient performance. *Transactions of ASME, Journal of Dynamic Systems, Measurement and Control*, *118*(4), 764–775.

Yao, B., & Tomizuka, M. (2001). Adaptive robust control of MIMO nonlinear systems in semi-strict feedback forms. *Automatica*, *37*(9), 1305–1321.

Chuxiong Hu is currently a direct Ph.D. student in Mechatronic Control Engineering at Zhejiang University in China, from which he received his B.Eng. degree in 2005. His research interests include coordinated motion control, precision mechatronics, adaptive control, robust control and nonlinear systems.

Bin Yao received his Ph.D. degree in Mechanical Engineering from University of California at Berkeley in February 1996 after obtaining the M.Eng. degree in Electrical Engineering from Nanyang Technological University, Singapore, in 1992, and the B.Eng. in Applied Mechanics from Beijing University of Aeronautics and Astronautics, China, in 1987. He has been with the School of Mechanical Engineering at Purdue University since 1996 and promoted to the rank of Professor in 2007. He was honored as a Kuang-piu Professor at the Zhejiang University in China in 2005.

Dr. Yao was awarded a Faculty Early Career Development (CAREER) Award from the National Science Foundation (NSF) in 1998 and a Joint Research Fund for Outstanding Overseas Chinese Young Scholars from the National Natural Science Foundation of China (NSFC) in 2005. He is the recipient of the O. Hugo Schuck Best Paper (Theory) Award from the American Automatic Control Council in 2004 and the Outstanding Young Investigator Award of ASME Dynamic Systems and Control Division (DSCD) in 2007. He has chaired numerous sessions and served in the International Program Committee of various IEEE, ASME, and IFAC conferences. From 2000 to 2002, he was the Chair of the Adaptive and Optimal Control Panel and, from 2001 to 2003, the Chair of the Fluid Control Panel of the ASME Dynamic Systems and Control Division (DSCD). He is currently the Chair of the ASME DSCD Mechatronics Technical Committee. He was a Technical Editor of the IEEE/ASME Transactions on Mechatronics from 2001 to 2005 and an Associate Editor of the ASME Journal of Dynamic Systems, Measurement, and Control from 2006 to 2009. More detailed information can be found at: https://engineering.purdue.edu/~byao

Qingfeng Wang received his Ph.D. and M.Eng. degrees in Mechanical Engineering from Zhejiang University, China, in 1994 and 1988 respectively. He then became a faculty at the same institution where he was promoted to the rank of Professor in 1999. He was the Director of the State Key Laboratory of Fluid Power Transmission and Control at Zhejiang University from 2001 to 2005 and currently serves as the Director of the Institute of Mechatronic Control Engineering. His research interests include the electro-hydraulic control components and systems, hybrid power system and energy saving technique for construction machinery, and system synthesis for mechatronic equipments.